NASA Contractor Report 4167

Modeling and Optimum Time Performance for Concurrent Processing

Roland R. Mielke, John W. Stoughton,
and Sukhamoy Som

NASA

NASA Contractor Report 4167

Modeling and Optimum Time Performance for Concurrent Processing

Roland R. Mielke, John W. Stoughton,
and Sukhamoy Som
Old Dominion University
Norfolk, Virginia

NASA

National Aeronautics
and Space Administration

Scientific and Technical
Information Division

1988

I. INTRODUCTION

The development of a new graph theoretic model for describing data and control flow associated with the execution of large-grained algorithms in a special distributed computing environment is presented. The model is identified by the acronym ATAMM which represents Algorithm To Architecture Mapping Model. The purpose of such a model is to provide a basis for establishing rules for relating an algorithm to its execution in a multiprocessor environment. Specifications derived from the model lead directly to the description of a data flow architecture. The availability of the ATAMM model is important for at least three reasons. First, it provides a context in which to investigate algorithm decomposition strategies without the need to specify a specific computer architecture. Second, the model identifies the data flow and control dialog required of any data flow architecture which implements the algorithm. Third, the model provides a basis for calculating analytically performance bounds for computing speed and throughout capacity.

The problem domain of the ATAMM model consists of decision free algorithms with computationally complex primitive operations which are assumed to be implemented in a dedicated data flow environment. The algorithms are such as may be found in (but not limited to) large scale signal processing and control applications. The anticipated multiprocessor environment is assumed to consist of two to twenty processing elements for concurrent execution of the various algorithm primitives.

The development of new computer architectures based upon distributed, multiprocessor organizations [1], [2] is motivated mainly by the requirement for increased speed and greater throughput capability in complex signal processing applications [3]. Recent advances in the production of

high-density microelectronics [4] has made possible the construction of parallel architectures consisting of identical, special purpose computing elements [5]. A number of models for describing the behavior of algorithms in this setting have been developed [6] - [8]. However, these models represent only the data flow and do not adequately display the complex issues of communication and control flow which must occur in any realization of the model. For this reason, it has been difficult to investigate how to effectively match the decomposition and scheduling of algorithms to the structure and control of parallel architectures. The importance of better understanding the relationship between algorithms and architectures is only now becoming recognized [9].

In Section II of the paper, the modeling process to describe algorithms in data flow architectures, ATAMM, is presented. The model consists of three Petri net marked graphs called the algorithm marked graph (AMG), the node marked graph (NMG), and the computational marked graph (CMG). In Section III, the operating characteristics of these graphs are investigated. A state variable description is presented and used to establish the graph properties of reachability, liveness, and safeness. Time performance measures for concurrent processing are defined in Section IV. The ATAMM model is used as the basis for calculating analytically lower bounds for these performance measures. Then in Section V, an operating strategy which achieves optimum time performance is developed. Several examples are presented to illustrate these concepts, and the results of experimental runs on actual multiprocessor hardware are reported.

II. ATAMM MODEL DEVELOPMENT

In this section the ATAMM model to describe concurrent processing of

decomposed algorithms is presented. The model consists of a set of Petri net marked graphs which incorporate general specifications of communication and processing associated with each computational event in a data flow architecture. First, a detailed description of the problem context is stated. This is followed by the definition of the ATAMM model consisting of the algorithm marked graph, the node marked graph, and the computational marked graph. Some familiarity with Petri nets [10] and marked graphs [11] is assumed in this presentation.

The problems of interest are decision-free, computationally complex problems as are often found in signal processing and control applications. A problem description normally results in the definition of a function given by the triple (X,Y,F). The set X represents the set of admissible inputs, the set Y represents the set of admissible outputs, and F:X->Y is the rule of correspondence which unambiguously assigns exactly one element from Y to each element of X. Associated with a computational problem is one or more algorithms. An algorithm is an explicit mathematical statement, expressed as an ordered set of primitive operations, which explains how to implement the rule of correspondence F. In general, a given problem can be decomposed by several different primitive operator sets. Also, for a given primitive operator set, there are often different orderings of primitive operations which can be specified to carry out the problem. Of special interest are algorithm decompositions in which two or more primitive operations can be performed concurrently. For such decompositions, the potential exists for decreasing the computational time required to execute the problem by making available a set of identical computational resources capable of implementing each of the primitive operations.

The hardware environment for executing the decomposed algorithms is assumed to consist of R identical processors or functional units (FUNs) where R has a value in the range of two to twenty. This range of resources is suggested for practical reasons due to the large-grained aspect of the algorithm decomposition and the need to maintain small communication times relative to process times. Each FUN is a processor having local memory for program storage and temporary input and output data containers. Each FUN can execute any algorithm primitive operation. The FUNs share a common global memory (GLM) which may be either centralized or distributed. The coordination of FUNs in relation to data and control flow is directed by the graph manager (GRM). The GRM also may be centralized or distributed. Output created by the completion of a primitive operation is placed into global memory only after the output data containers have been emptied. That is, outputs must be consumed as inputs to successor primitive operations before allowing new data to fill the output locations. Assignment of a functional unit to a specific algorithm primitive operation is made by the GRM only when all inputs required by the operation are available in global memory and a functional unit is available.

An algorithm marked graph is a marked graph which represents a specific algorithm decomposition. Vertices of the algorithm graph are in a one-to-one correspondence with each occurrence of a primitive operation. The algorithm graph contains an edge (i,j) directed from vertex i to vertex j if the output of primitive operation i is an input for primitive operation j. Edge (i,j) is marked with a token if an output from primitive operator i is available as an input to primitive operator j. When constructing an algorithm graph, vertices (primitive operations) are displayed as circles, and edges (input-output signals) are displayed as directed line segments

4

connecting appropriate vertices. The presence of a token on an edge is indicated by a solid dot placed on the edge. Source transitions and sink transitions for input and output signals are represented as squares. Sources for constants are not usually included in the algorithm marked graph; however, triangles are used for this purpose when necessary.

To illustrate the construction of an algorithm marked graph, consider the problem of computing the output of a discrete linear system given a sequence of inputs to the system. Let the system be described by the state equation

$$x(k) = Ax(k-1) + Bu(k)$$

and output equation

$$y(k) = Cx(k).$$

where x is a p-vector, u is an m-vector, and y is an r-vector. The primitive operations are defined as matrix multiplication and vector addition, and the natural algorithm decomposition resulting from the state equation description is selected. The algorithm marked graph for this decomposed algorithm is shown in Figure 1. The initial marking indicates that initial condition data are available.

The algorithm marked graph is a useful tool for representing decomposed algorithms and for displaying data flow within an algorithm. However, the algorithm graph does not display procedures that a computing structure must manifest in order to perform the computing task. In addition, the issues of control, time performance, and resource management are not apparent in this graph. These important aspects of concurrent processing are included in the ATAMM model through the definition of two additional graphs. The node marked graph (NMG) is defined to model the execution of a primitive

5

operation. The computational marked graph, obtained from the AMG and the NMG by a set of construction rules, integrates both the algorithm requirements and the computing environment requirements into a comprehensive graph model. These additional marked graphs are defined in the following.

The NMG is a Petri net representation of the performance of a primitive operation by a functional unit. Three primary activities, reading of input data from global memory, processing of input data to compute output data, and writing of output data to global memory, are represented as transitions (vertices) in the NMG. Data and control flow paths are represented as places (edges), and the presence of signals is notated by tokens marking appropriate edges. The conditions for firing the process and write transitions of the NMG are as defined for a general Petri net, while the read transition has one additional condition for firing. In addition to having a token present on each incoming signal edge, a functional unit must be available for assignment to the primitive operation before the read node can fire. Once assigned, the functional unit is used to implement the read, process, and write operations before being returned to a queue of available FUNs. The initial marking for an NMG consists of a single token in the "process ready" place. The NMG model is shown in Figure 2.

A computational marked graph (CMG) is constructed from the AMG and the NMG by the following rules.

1. Source and sink nodes in the algorithm marked graph are represented by source and sink nodes in the CMG.

2. Nodes corresponding to primitive operations in the algorithm marked graph are represented by NMGs in the CMG.

3. Edges in the algorithm marked graph are represented by edge pairs, one forward directed for data flow and one backward directed for

control flow, in the CMG. The initial marking for the edge pair consists of a single token in the forward-directed place if data are available, or a single token in the backward-directed place if data are not available.

The play of the CMG proceeds according to the following graph rules.

1) A node is enabled when all incoming edges are marked with a token. An enabled node fires by encumbering one token from each incoming edge, delaying for some specified transition time, and then depositing one token on each outgoing edge.

2) A source node and a sink node fire when enabled without regard for the availability of a FUN.

3) A primitive operation is initiated when the read node of an NMG is enabled and a FUN is available for assignment to the NMG. A FUN remains assigned to an NMG until completion of the firing of the write node of the NMG.

In order to illustrate the construction of a computational marked graph, the CMG corresponding to the algorithm marked graph of Figure 1 is shown in Figure 3. The computational marked graph is useful because it clearly displays the data and control flow which must occur in any hardware implementation of the model process, and because it provides a hardware independent context in which to evaluate process performance.

The complete ATAMM model consists of the algorithm marked graph, the node marked graph, and the computational marked graph. A pictoral display of this model is shown in Figure 4. In the next section, important operating characteristics of the ATAMM model are investigated.

III. MODEL CHARACTERISTICS

In the previous section, a marked graph model consisting of the AMG, the NMG, and the CMG is defined as a means to describe concurrent processing of decomposed algorithms. In this section the ATAMM model is studied analytically to determine important graph operating characteristics. First, a state description which expresses the next graph marking as a function of the present marking and a vector indicating which transition is to be fired is developed. Then, the marked graph properties of reachability, liveness, and safeness are considered for the CMG. Two excellent papers by Murata [11], [12] on properties of marked graphs are the source for much of the material presented in this section.

Let G be a marked graph consisting of m places and n transitions. The m-vector M_k denotes the marking vector for G resulting from the firing of some sequence of k transitions. The following two definitions are necessary to develop the state description of the CMG.

Definition 1: Complete Incidence Matrix. The complete incidence matrix for a marked graph G is the (nxm) matrix $A = [a_{ij}]$ having rows corresponding to transitions, columns corresponding to places, and where

$$a_{ij} = \begin{cases} +1(-1) & \text{if place j is incident at transition i} \\ & \text{and directed out of (into) the transition} \\ 0 & \text{if place j is not incident at transition j} \end{cases}$$

Definition 2: Elementary Firing Vector. An elementary firing vector u_k is an n-vector having all zero entries except for the ith component which is 1 denoting that transition i is the kth transition to fire in some transition firing sequence.

To gain insight to the state equation description, it is helpful to

consider the firing of transition k. If $a_{ki} = -1(+1)$, place i is an input (output) place to transition k. Therefore, transition k is enabled if $M(i) = 1$ for each input place. When transition k fires, one token is removed from each input place and one token is added to each output place. These observations lead to the following next state description for a marked graph.

Property 1: Next State Description. For a marked graph G with present marking vector M_{k-1} and elementary firing vector u_k, the next marking vector is given by

$$M_k = M_{k-1} + A^T u_k.$$

The next state description can be used to express the graph marking resulting from the application of sequences of elementary firing vectors. This is done in the next definition and property.

Definition 3: Firing Count Vector. Let $(u_1, u_2, \ldots, u_d)$ be a sequence of elementary firing vectors taking a marked graph G from an initial marking M_0 to a destination marking M_d. The firing count vector x_d for this firing sequence is defined by

$$x_d = \sum_{k=1}^{d} u_k.$$

Property 2: State Equation Description. For a marked graph G with initial marking vector M_0, the marking vector resulting from the application of elementary firing vector sequence $(u_1, u_2, \ldots, u_d)$ is given by

$$M_d = M_0 + A^T x_d.$$

Using the state description of a marked graph as a basis, the property of reachability is investigated. Necessary and sufficient conditions for a CMG marking vector to be reachable from an initial marking are established, and it is shown that the number of tokens contained in any directed circuit of the CMG is invariant under transition firings.

Definition 4: Reachability. A marking M_d is reachable from an initial marking M_0 if there exists a sequence of elementary firing vectors that transforms M_0 to M_d.

The following definition is required to state the reachability conditions for a CMG.

Definition 5: Fundamental Circuit Matrix. Let T be a tree of a connected marked graph G. The set of (m-n+1) circuits, each uniquely formed by appending one cotree edge to the tree, is called the set of fundamental circuits of G for tree T [13]. The fundamental circuit matrix for G for tree T is the (m-n+1) x (m) matrix $B_f = [b_{ij}]$ having rows corresponding to fundamental circuits, columns corresponding to places, and where

$$b_{ij} = \begin{cases} +1(-1) & \text{if place j is contained in f-circuit i and} \\ & \text{the place and circuit directions agree} \\ & \text{(disagree)} \\ \\ 0 & \text{if place j is not contained in f-circuit i.} \end{cases}$$

Property 3: Reachability in the CMG. In a computational marked graph G, a marking M_d is reachable from an initial marking M_0 if and only if $B_f M_d = B_f M_0$, where B_f is a fundamental circuit matrix for G.

Proof. It is shown in [11] (Theorem 3) that the property is true for marked graphs containing no token-free directed circuits. By the construction rules for the CMG, directed circuits occur in exactly four ways. First, each NMG consists of a directed circuit which contains an initial marking token in the "process ready" place. Second, a directed circuit is formed each time an NMG is linked to another NMG. Since one of the two linking places contains an initial marking token and both places are contained in the circuit, this circuit is never token free. Third, directed circuits exist in the CMG corresponding to interconnected feedforward paths in the algorithm marked graph. Each such circuit contains one or more backward-directed control edge containing one initial marking token. Fourth, directed circuits exist in the CMG corresponding to directed circuits in the algorithm marked graph. Each such circuit contains exactly one forward-directed edge containing one initial marking token representing initial condition data. Therefore, the CMG contains no token-free directed circuits and the property follows.

As a direct consequence of the reachability property of the CMG, it can be shown that the number of tokens in any directed circuit is constant. This characteristic is stated as Property 4.

Property 4: Token Count Invariance. In a CMG, the number of tokens contained in a directed circuit is invariant under transition firing.

Proof. Consider a directed circuit C of a CMG. The entries in the row of a circuit matrix B corresponding to C are +1 in columns representing edges in C and are 0 otherwise. If M is a marking vector, the component of BM corresponding to C is equal to the number of tokens in directed circuit C under marking M. Therefore, if M_d is any marking reachable from an initial marking M_0, it follows from Property 3 that $BM_d = BM_0$. That is, the number of

tokens in directed circuit C under initial marking M_0 is equal to the number of tokens under any marking M_d reachable from M_0. This completes the proof.

Next, liveness and a closely related property called consistency are considered. It is shown that the CMG is live and consistent.

Definition 6: Liveness. A marked graph G is said to be live for a marking M if, for all markings reachable from M, it is possible to fire any transition of G by progressing through some transition firing sequence.

Property 5: Liveness in the CMG. The computational marked graph is live for all appropriate initial marking vectors.

Proof. It is shown in [12] (Property 2) that a marked graph G is live for a marking M if and only if G contains no token-free directed circuits in marking M. As stated in the proof of Property 3, for all appropriate initial markings M_0, the CMG contains no token-free directed circuits. Therefore, the property follows.

Definition 7: Consistency. A marked graph G is said to be consistent if there exists a marking M and a transition firing sequence S from M back to M such that every transition occurs at least once is S.

Property 6: Consistency in the CMG. A connected computational marked graph G is consistent. In addition, each transition of G occurs an equal number of times in a firing sequence from a marking M back to M.

Proof. From Property 2, if a CMG is consistent, then there exists a marking $M_d = M_0$ and a firing count vector $x_d > 0$ such that $A^T x_d = 0$. The converse is also true. The incidence matrix for a marked graph G is an (n x m) matrix A. If G is connected, then it is known [13] that the rank of A is n-1, and thus the null space of A^T has dimension one. It is observed that

each row of A^T has one (1), one (-1), and all remaining terms are (0). Therefore, if C_j denotes the jth column of A^T, it follows that

$$\sum_{j=1}^{n} C_j = 0.$$

Thus, there exists a vector $x_d = [k \ k \ \ldots \ k]^T$, $k > 0$, which uniquely satisfies $A^T x_d = 0$. This completes the proof.

The final graph property considered in this section is safeness. This property is first defined, and then it is shown that CMG is safe.

Definition 8: Safeness. A marked graph G is said to be safe for marking M if, for all markings reachable from M, no place contains more than one token.

Property 7: Safeness in the CMG. The computational marked graph is safe for all appropriate initial marking vectors.

Proof. By Property 4, the token count for each directed circuit of the CMG is invariant under transition firing. Therefore it is sufficient to show that each edge of the CMG belongs to at least one directed circuit containing a single token. By the construction rules for the CMG, all CMG edges can be classified into two groups, NMG edges and linking edges. NMG edges occur in groups of three and always form a directed circuit containing one token. Linking edges occur in pairs, one forward directed and one backward directed, and also form a directed circuit with the forward directed edges of the NMG. One of the linking edges, but not both, always contains one token while the forward directed edges of the NMG contain no tokens.

Therefore, each edge of the CMG is contained in a directed circuit with one token, and the property follows.

IV. PERFORMANCE ANALYSIS

The importance of the ATAMM model is that it establishes a context in which to investigate the performance of decomposed algorithms in multiprocessor data flow architectures. In this section, performance measures indicating computing speed and throughput capacity are defined. Bounds for these quantities are calculated analytically from the algorithm marked graph and the computational marked graph. This information is essential for efficiently matching algorithm decompositions with architecture implementations. The work presented in this section is an interesting application and extension of recent investigations of the performance of Petri nets [14], [15] and marked graphs [16].

It is assumed that a decomposed algorithm is implemented in a multiprocessor architecture containing R computing resources or functional units. Each functional unit is capable of performing any of the primitive operations whose sequence defines the decomposition. A computational task consists of completing the algorithm for one frame of data and is initiated when an input data token from the source node is encumbered. Task output occurs when a corresponding output data token is deposited at the output sink node. A task is completed when all computing associated with the task is completed. It should be noted that task output and task completion do not always coincide. In many iterative signal processing algorithms, computing to generate initial conditions for the next iteration often occurs after an output has been calculated. Task completion is usually indicated in the AMG or CMG by the return of the graph to some steady-state initial

14

marking. To facilitate measurement of throughput capacity, it is assumed that tasks are repeated periodically with new input data sets. New data sets are available continuously as input tokens from the input source node. Included in this problem class are iterative algorithms where the present task requires as inputs data from previous task calculations.

Concurrency in this problem setting occurs in two ways. First, different functional units may perform simultaneously several primitive operations belonging to a single task. This type of concurrency is referred to as vertical concurrency. Vertical concurrency has a direct effect on task computing speed. It is limited by the number of primitive operations that can be performed simultaneously in a given algorithm decomposition, and by the number of functional units available to perform the primitive operations. Second, different functional units may perform simultaneously primitive operations belonging to different tasks sequentially input to the computing system. Called horizontal concurrency, this type of concurrency has a direct effect on throughput capacity. It is limited by the capacity of the graph to accommodate additional task inputs, and by the number of functional units available to implement the tasks. In the following it is shown that the process of algorithm decomposition imposes bounds on the amount of vertical concurrency and horizontal concurrency possible in a given problem. If sufficient computing resources are available, operation at these bounds can be achieved. If the number of computing resources is limited, the bounds cannot be reached simultaneously and trade-offs between the amount of vertical concurrency and horizontal concurrency are possible.

Three performance measures for concurrent processing are defined. The first two parameters, TBIO and TT, are indicators of computing speed and reflect the degree of vertical concurrency. The third parameter, TBO, is a

15

measure of throughput capacity and thus reflects the degree of horizontal and vertical concurrency.

Definition 9: TBIO. The performance measure TBIO is the computing time which elapses between a task input and the corresponding task output.

Definition 10: TT. The performance measure TT is the computing time which elapses between a task input and the completion of all computation associated with that task.

Definition 11: TBO. The performance measure TBO is the computing time which elapses between successive task outputs when the graph is operating periodically in steady-state.

The remainder of this section is devoted to developing lower bounds for these performance measures.

Let G denote an algorithm marked graph representing a decomposed algorithm. The lower bound for TBIO is the shortest time required for a data token from the data input source to propagate through the graph to the data output sink. Similarly, the lower bound for TT is the shortest time required to complete all computing activity initiated by the injection of a data input source. These shortest times are the actual performance times when only a single task is active in the graph during any time interval (no horizontal concurrency), and as many computing resources as are required are available (maximum vertical concurrency). Under these operating conditions, lower bounds for TBIO and TT are calculated by identifying certain longest paths in a graph obtained from the algorithm marked graph. This new graph, called the modified algorithm graph G_M, is defined and then used to determine lower bounds for TBIO and TT.

Definition 12: Modified Algorithm Graph. Let p_i be a place of G, directed from transition t_r to transition t_s, which contains a token of the initial

marking. The modified algorithm graph G_M is obtained from the graph G by the following construction rules.

1. Place p_i is deleted from G.

2. A new place p_{i1}, directed from the data input source to transition t_s, is added to G.

3. A new output sink s_i different from all other output sinks, and a new place p_{i2}, directed from transition t_r to s_i, are added to G.

4. The above rules are repeated for each place of G containing a token of the initial marking.

Lower bounds for TBIO and TT are presented in Theorem 1 and Theorem 2 respectively.

Theorem 1: Lower Bound for TBIO. Let P_i be the ith directed path in G_M from the data input source to the data output sink, and let $T(P_i)$ denote the sum of transition times for transitions contained in P_i. Then,

$$TBIO_{LB} = Max \ \{T(P_i)\},$$

where the maximum is taken over all paths P_i in graph G_M.

Proof. Without loss of generality, let t_f be the last transition in all paths P_i directed from the data input source to the data output sink. Transition t_f is enabled when each input place for t_f contains a token. Since by assumption a computing resource is available, t_f fires as soon as it becomes enabled. Let p_q be the last input place for t_f to acquire a token, and let t_g be the input transition for place p_q. Continuing this labeling procedure results in a backward path construction process. This process is repeated, first at t_g, and then at each succeeding transition

17

until the data input source is reached, identifying a path P_j. By the construction process for the path, it is clear that $T(P_j) = \text{Max } \{T(P_i)\}$, where the maximum is over all paths P_i in G_M. It is also clear that $TBIO_{LB}$ can be no shorter than $T(P_j)$ so that $TBIO_{LB} \geq T(P_j)$. Since a computing resource is available when each transition in P_j is enabled, the time between input and corresponding output can be no longer than $T(P_j)$ so that $TBIO_{LB} \leq T(P_j)$. Therefore, $TBIO_{LB} = T(P_j) = \text{Max } \{T(P_i)\}$, where the maximum is over all paths P_i in G_M. This completes the proof.

Theorem 2: Lower Bound for TT. Let P_i be the ith directed path in G_M from the data input source to any output sink, and let $T(P_i)$ denote the sum of transition times of transitions contained in P_i. Then,

$$TT_{LB} = \text{Max } \{T(P_i)\}$$

where the maximum is taken over all paths P_i in graph G_M.

Proof. By the construction rules for graph G_M, a task is initiated when input data tokens are input from the data input source, and is completed when all output sinks have accepted tokens. Therefore, TT is the time which elapses from injection of input tokens to the arrival of a token at the last fired output sink. Let $T(P_t) = \text{Max}\{T(P_i)\}$, P_i in G_M, be the longest path time of paths from the data input source s_I to any output sink, say s_t. Since a token must reach sink s_t before a task is completed, it follows that $TT_{LB} \geq T(P_t)$. Since a resource is available for each transition to fire when enabled, and since P_t is the longest path in G_M, it also follows that $TT_{LB} \leq T(P_t)$. Therefore, $TT_{LB} = T(P_t) = \text{Max}\{T(P_i)\}$, where the maximum is over all paths P_i in G_M. This completes the proof.

18

To illustrate the application of Theorem 1 and Theorem 2, $TBIO_{LB}$ and TT_{LB} are computed for the algorithm graph shown in Figure 1. For this example, the following transition times are assumed: $T(1) = 4$, $T(2) = 1$, $T(3) = 5$, and $T(4) = 6$. The modified algorithm graph corresponding to Figure 1 is shown in Figure 5. The modified algorithm graph contains two paths directed from the data input source s_I to the data output sink s_0. Path P_1 consists of edge set $\{1, 2, 3, 4\}$ with $T(P_1) = 10$, and path P_2 consists of edge set $\{5\text{-}1, 3, 4\}$ with $T(P_2) = 6$. Therefore, since $T(P_1) > T(P_2)$, path P_1 determines the lower bound for TBIO and $TBIO_{LB} = 10$. The modified algorithm graph contains two additional directed paths from the data input source s_I to the output sink s_5. Path P_3 consists of edge set $\{1, 2, 6, 5\text{-}2\}$ with $T(P_3) = 11$, and path P_4 consists of edge set $\{5\text{-}1, 6, 5\text{-}2\}$ with $T(P_4) = 7$. Since $T(P_3) > T(P_1) > T(P_4) > T(P_2)$, path P_3 determines the lower bound for TT and $TT_{LB} = 11$.

Next a lower bound for the performance measure TBO is presented. Let G be a computational marked graph representing a decomposed algorithm. It is assumed that operating conditions for G are set to maximize horizontal concurrency. That is, data tokens are continuously available at the data input source, and as many computing resources as needed can be called to perform primitive operations. With these conditions, the graph plays periodically in steady-state, and TBO_{LB} is the shortest time possible between successive outputs.

Theorem 3: Lower Bound for TBO. Let G be a computational marked graph and let C_i be the ith directed circuit in G. The notation $T(C_i)$ denotes the sum of transition times of transitions contained in C_i, and $M(C_i)$ denotes the number of tokens contained in C_i. Then,

$$TBO_{LB} = Max \{T(C_i)/M(C_i)\},$$

where the maximum is taken over all directed circuits in G.

Proof. Without loss of generality, let t_f be the output transition in G so that an output is produced each time t_f completes firing. Then TBO_{LB} is the minimum firing period of transition t_f. By Property 6, G is consistent so that all transitions of G fire periodically with minimum period TBO_{LB}. It is shown in [12] (pp. 58-60) that the minimum firing period of each transition of a marked graph is given by $Max\{T(C_i)/M(C_i)\}$, where the maximum is taken over all directed circuits C_i in G. Therefore, the theorem follows.

The computational marked graph shown in Figure 3 is used to illustrate Theorem 3. This CMG contains many directed circuits. However, the directed circuit which contains all NMG nodes of transitions 2 and 4 contains only one token and maximizes the ratio $T(C_i)/M(C_i)$. Therefore, the shortest time possible between successive outputs in this graph is $TBO_{LB} = 7$. In the next section, a strategy for achieving optimum time performance is investigated.

V. STRATEGY FOR OPTIMUM TIME PERFORMANCE

A model describing decomposed algorithms for implementation in a distributed data flow architecture is described in Sections II and III, and performance measures are defined in Section IV. An important problem remaining is to develop an operating strategy for the ATAMM model which achieves optimum time performance with a minimum number of computing resources. Unfortunately, this problem is equivalent to a class of scheduling problems which is known to be NP-complete. Thus, there exists no algorithm for obtaining an optimum solution which is better than enumerating all possible solutions and then choosing the best one. However, an

20

important suboptimal operating strategy which achieves optimum time performance, but possibly requires more than the minimum number of computing resources, has been developed. This strategy is presented and illustrated by example in this section.

When presented with continuously available input data sets, the natural behavior of a data flow architecture results in operation where new data sets are accepted as rapidly as the available resources permit. That is, the architecture naturally operates at high levels of horizontal concurrency with the possible loss of capability for achieving high levels of vertical concurrency. This results in performance characterized by high throughput rates, $TBO=TBO_{LB}$, but relatively poor task computing speed so that $TBIO \gg TBIO_{LB}$ and $TT \gg TT_{LB}$. In many signal processing and control applications, it is important to achieve both high throughput rate and high task computing speeds. Often, designers are willing to provide extra hardware to realize optimum time performance. The suboptimal operating strategy presented in this section results in performance having the following characteristics.

1. When $R > R_{Max}$, operation achieves $TBIO_{LB}$, TT_{LB}, and TBO_{LB}. R_{Max} is computed in implementing the strategy, and represents the minimum number of resources which insures maximum horizontal concurrency and maximum vertical concurrency under this strategy.

2. When $R_{Max} > R > R_{Min}$, operation achieves $TBIO_{LB}$ and TT_{LB}, but $TBO > TBO_{LB}$. The strategy preserves task computing speed or vertical concurrency at the expense of throughput rate or horizontal concurrency. R_{Min} is also computed in implementing the strategy, and represents the minimum number of resources needed to maintain vertical concurrency with limited horizontal concurrency.

3. When $R_{Min} > R > 1$, operation continues but performance degrades so

21

that $TBIO > TBIO_{LB}$, $TT > TT_{LB}$, and $TBO > TBO_{LB}$.

Implementation of the operating strategy is illustrated in Figure 6. All that is required is to limit the rate at which new input data are presented to the CMG. This is accomplished by adding a control transition connected in a directed circuit with the data input source. The control transition imposes a minimum delay of D time units between inputs. Delay D is chosen according to the following rule:

$$D = \begin{cases} TBO_{LB} & R > R_{Max} \\ TBO_{Min} & R_{Max} > R > R_{Min} \\ TCE & R_{Min} > R > 1. \end{cases}$$

TCE denotes the total computing effort required to complete the task, and TBO_{Min}, R_{Max}, and R_{Min} are computed as part of the strategy design procedure.

The operating strategy design process consists of five steps. These steps are presented and explained in the remainder of this section. An operating strategy is developed for the example algorithm graph shown in Figure 7 to illustrate each step as it is presented.

Step 1. Choose a convenient transition firing rule. A rule to determine when an enabled transition in the CMG fires must be specified. A natural rule is to specify that enabled transitions fire when a computing resource is available . If conflict exists, such as when there are more enabled transitions than computing resources, then firing occurs according to a priority ordering of the transitions. For the example algorithm graph, the highest to lowest priority ordering of the transitions is chosen as (5,4,3,-7,2,6,1).

Step 2. Determine TBO_{LB}. The performance bound TBO_{LB} is found from the

computational marked graph by application of Theorem 3. The CMG correspond-
ing to the example algorithm graph is shown in Figure 8. The directed cir-
cuit identified in this figure contains 6 transition time units and 2 to-
kens, and maximizes the ratio $T(C_i)/M(C_i)$ for all directed circuits. There-
fore, $TBO_{LB} = 3$.

Step 3. Determine the resource utilization envelope of a single task re-
quired for maximum vertical concurrency at steady-state with $TBO = TBO_{LB}$.
The purpose of this step is to determine the number of computing resources
required as a function of time to achieve maximum vertical concurrency in a
single task. The envelope is determined by playing the graph assuming un-
limited resources and an input rate of TBO_{LB} until steady-state operation is
reached. The resource utilization envelope is obtained by counting the
number of computing resources used for a single task during each time inter-
val. The play of the example algorithm graph under these conditions is
shown in Figure 9, and the resulting resource utilization envelope is shown
in Figure 10.

Step 4. Stabilize the resource utilization envelope by adding control
places as necessary. If the time between inputs to the CMG is increased
above TBO_{LB}, the resource utilization envelope may change from that observed
in Step 3. Since knowledge of the envelope is required to calculate the
number of required resources, additional places are appended to the AMG and
the CMG to freeze the shape of the envelope. For example, the play of the
example algorithm graph of Figure 8 with an injection time of 4 is shown in
Figure 11. At this slower injection rate, transition 6 fires one time unit
earlier. To prevent time movement of transition 6, a control place directed
from transition 2 to transition 6 is added. This place prevents the firing
of transition 6 until transition 2 has completed firing. Thus the resource

23

utilization envelope computed for an input period of TBO_{LB} is the envelope for all input periods $TBO > TBO_{LB}$.

Step 5. Compute R_{Max}, R_{Min}, and $TBO_{Min}(R)$ using the resource utilization envelope. R_{Max} is determined by overlaying resource utilization requirements, each delayed by TBO_{LB} with respect to the previous one, as shown in Figure 12 for the example. R_{Max} is equal to the largest resource requirement during any time interval within the steady state operating period. R_{Min} is the minimum number of resources necessary to insure maximum vertical concurrency with no horizontal concurrency. This number is equal to the maximum resource requirement indicated in the resource utilization envelope for a single task. For the example problem, R_{Max} = 5 and R_{Min} = 3. The value of TBO_{Min} for each resource number R between R_{Max} and R_{Min} inclusive, is determined by increasing the delay between overlapping resource utilization envelopes until the maximum resource requirement is R. TBO_{Min} is the smallest input delay to produce this resource requirement. For the example, the calculations of TBO_{Min} for R = 4 and R = 3 are illustrated in Figure 13 and Figure 14 respectively. The results of these calculations are $TBO_{Min}(4)$ = 3.5 and $TBO_{Min}(3)$ = 4.

The performance of the example algorithm graph is summarized in Figure 15. Optimum time performance of $TBIO_{LB} = TT_{LB} = 7$ and $TBO_{LB} = 3$ is achieved for $R > R_{Max}$ = 5. At R = 4, TBIO and TT remain at the optimum values and TBO_{Min} decreases to 3.5. At R = 3, TBIO and TT again remain at the optimum values and TBO_{Min} decreases to 4. For values of R below R_{Min}, time performance generally degrades. However, in this example TBIO and TT remain at 7 for R = 2, while TBO_{Min} decreases to 6. Finally, at R = 1, performance degrades to TBIO = TT = TBO = TCE = 10. Another perspective of algorithm

performance is shown in Figure 16. This figure displays throughput rate, (1/TBO), as a function of the number of functional units R. The peak height of each bar indicates the maximum throughput rate which can be achieved with the indicated number of processors. The bars also indicate more clearly that operation at any throughput rate less than maximum is possible for a given number of functional units. This design procedure is easily applied to much larger algorithm graphs more representative of actual signal processing and control problems.

VI. CONCLUSION

A new model useful for understanding the relationship between decomposed algorithms and data flow architectures has been presented. Named ATAMM for Algorithm to Architecture Mapping Model, the model consists of Petri net marked graphs called the algorithm marked graph, the node marked graph, and the computational marked graph. After establishing that the computational marked graph is live, safe and consistent, graph time performance measures of time between input and output (TBIO), task time (TT), and time between outputs (TBO) were defined. Then lower bounds for the performance measures were calculated analytically from the modified algorithm graph and the computational marked graph. A design strategy for achieving optimum time performance was proposed and illustrated with a design example.

Simulation tools and an actual hardware prototype have been developed to test and validate the ATAMM model. The simulation software package [17] consists of a PC-based computer model of the CMG. Algorithms are entered to the package by specifying the algorithm marked graph, and simulation output consists of a graphical display of the movement of tokens. An accompanying diagnostic software package [18] automatically computes and displays

performance measures and other performance data. A hardware prototype [19] has also been constructed to validate the ATAMM operating rules and to provide a benchmark for testing the simulation software. The architecture is shown in Figure 17 and is one of several candidates which could be used to perform concurrent operations according to the ATAMM rules. A primary motivation for this particular design was the availability of hardware. The system consists of S-100 crates having a 16-bit CPU card, multiple serial I/O channels, and 32K memory. A personal computer is used to host the system and to down load algorithm graph descriptions to the system. A number of decomposed algorithms, including those presented here, have been investigated using these tools.

Continuing research is designed to generalize the ATAMM model and is focused in three main areas. The present model assumes that all functional units are identical and that each is able to perform all primitive operations. An important extension is to model the situation where there are two or more different groupings of processors where each group is able to perform only a subset of the required primitive operations. The present model represents only decision-free algorithms. Another important extension is to develop the capability to admit algorithms containing data-dependent branching points. Finally, methods for decomposing algorithms which result in good performance are being studied in the context of the ATAMM model.

REFERENCES

1. P. Treleaven, D. Brownbridge and R. Hopkins, "Data-driven and demand-driven computer architectures," Computing Surveys, vol. 14, pp. 93-143, March 1982.

2. V. Srini, "An architectural comparison of dataflow systems," Computer, pp. 68-88, March 1986.

3. W. Rheinbolt, "Report of the panel on future directions in computational mathematics, algorithms, and scientific software," Sponsored by NSF Grant DMS-85-3483, SIAM, 1985.

4. T. Longo, G. Herzog and D. Maxwell, "A fast single chip 1750A CPU and compatible support components in VHSIC-size CMOS technology," Proceedings of the Government Microcircuit Applications Conference, pp. 317-320, 1986.

5. W. Wehner, W. Everhart, S. Shankar and K. Stalsberg, "A VSHIC architecture for highly parallel image understanding," Proceedings of the Government Microcircuit Applications Conference, pp. 117-120, November 1986.

6. M. Sowa and T. Murata, "A data flow computer architecture with program and token memories," IEEE Transactions on Computers, vol. 31, pp.820-824, September 1982.

7. K. Kavi, B. Buckles and U. Narayan Bhat, "A formal definition of data flow graph models," IEEE Transactions on Computers, vol. 35, pp. 940-948, November 1986.

8. M. Granski, I. Koren and G. Silberman, "The effect of operation scheduling on the performance of a data flow computer," IEEE Transactions on Computers, vol. 36, pp. 1019-1029, September 1987.

9. L. Jamieson, H. Siegel, E. Delp and A. Whinston, "The mapping of parallel algorithms to reconfigurable parallel architectures," Proceedings of Future Directions in Computer Architecture and Software, D. Agrawal Ed., ARO Contract DAAG29-81-D-0100, pp. 147-154, May 1986.

10. J. Peterson, <u>Petri Net Theory and the Modeling of Systems</u>, Englewood Cliffs, N.J.: Prentice-Hall, 1981.

11. T. Murata, "Circuit theoretic analysis and synthesis of marked graphs," IEEE Transactions on Circuits and Systems, vol. 24, pp. 400-405, July 1977.

12. T. Murata, "Modeling and analysis of concurrent systems," Handbook of Software Engineering, C. Vick and C. Ramamoorthy Editors, pp. 39-63, Van Nostrand Reinhold, 1984.

13. S. Seshu, and M. Reed, Linear Graphs and Electrical Networks, Addison-Wesley Publishing Co., Inc, 1961.

14. J. Sifakis, "Performance evaluation of systems using nets," Net Theory and Applications, W. Brauer Editor, pp. 307-319, Springer-Verlag, 1979.

15. C. Ramamoorthy and G. Ho, "Performance evaluation of asynchronous concurrent systems using Petri nets," IEEE Transactions on Software Engineering, vol. 6, pp. 440-449, September 1980.

16. T. Murata, "Synthesis of decision-free concurrent systems for prescribed resources and performance," IEEE Transactions on Software Engineering, vol. 6, pp. 525-530, November 1980.

17. K. Jackson, R. Tymchyshyn, R. Mielke and J. Stoughton, "Simulation software for concurrent processing," Proceedings of the IEEE Southeastcon Conference, pp. 82-86, April 1987.

18. R. Obando, "Simulation software for performance evaluation of concurrent processing," Master's Thesis, Old Dominion University, Norfolk, Virginia, October 1987.

19. J. Stoughton and R. Mielke, "Petri net model for concurrent processing of complex algorithms," Proceedings of the Government Microcircuit Applications Conference, pp. 11-14, November 1986.
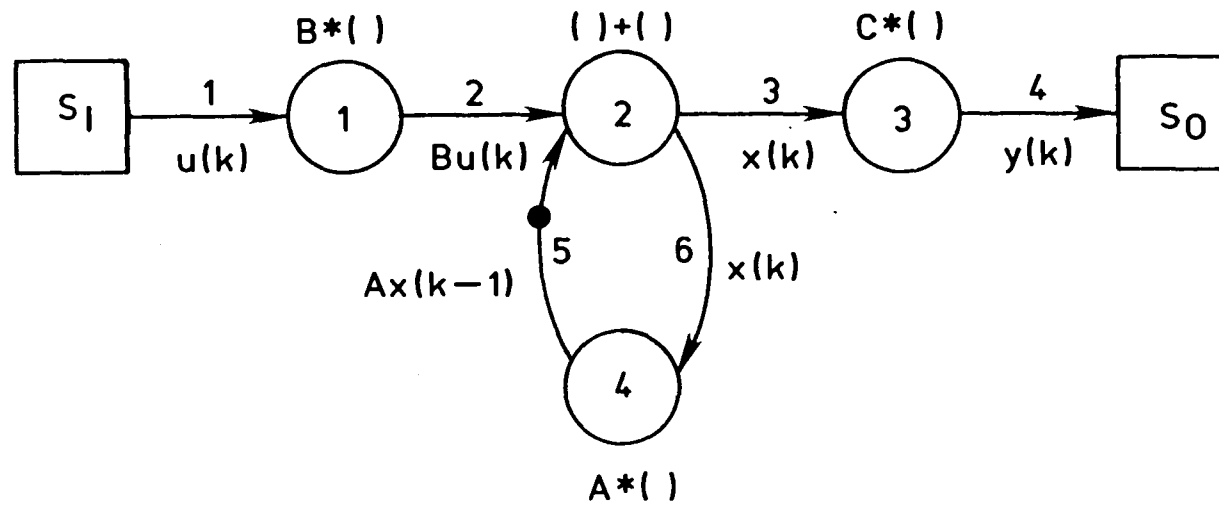
Figure 1. Algorithm marked graph for discrete system equation.
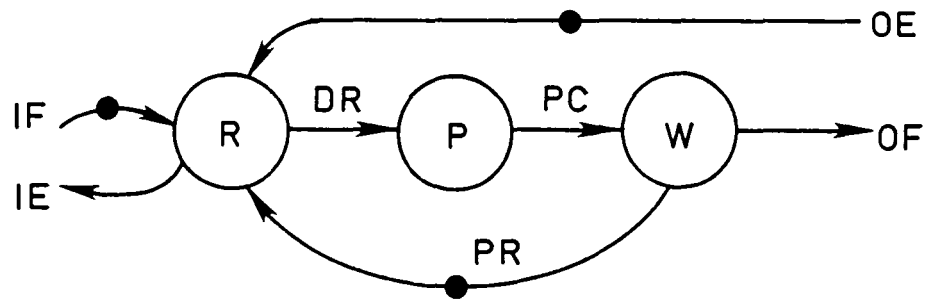
NMG EDGE LABELS

IF	Input Buffer Full
IE	Input Buffer Empty
DR	Data Read
PC	Process Complete
PR	Process Ready
OE	Output Buffer Empty
OF	Output Buffer Full

Figure 2. ATAMM node marked graph model.
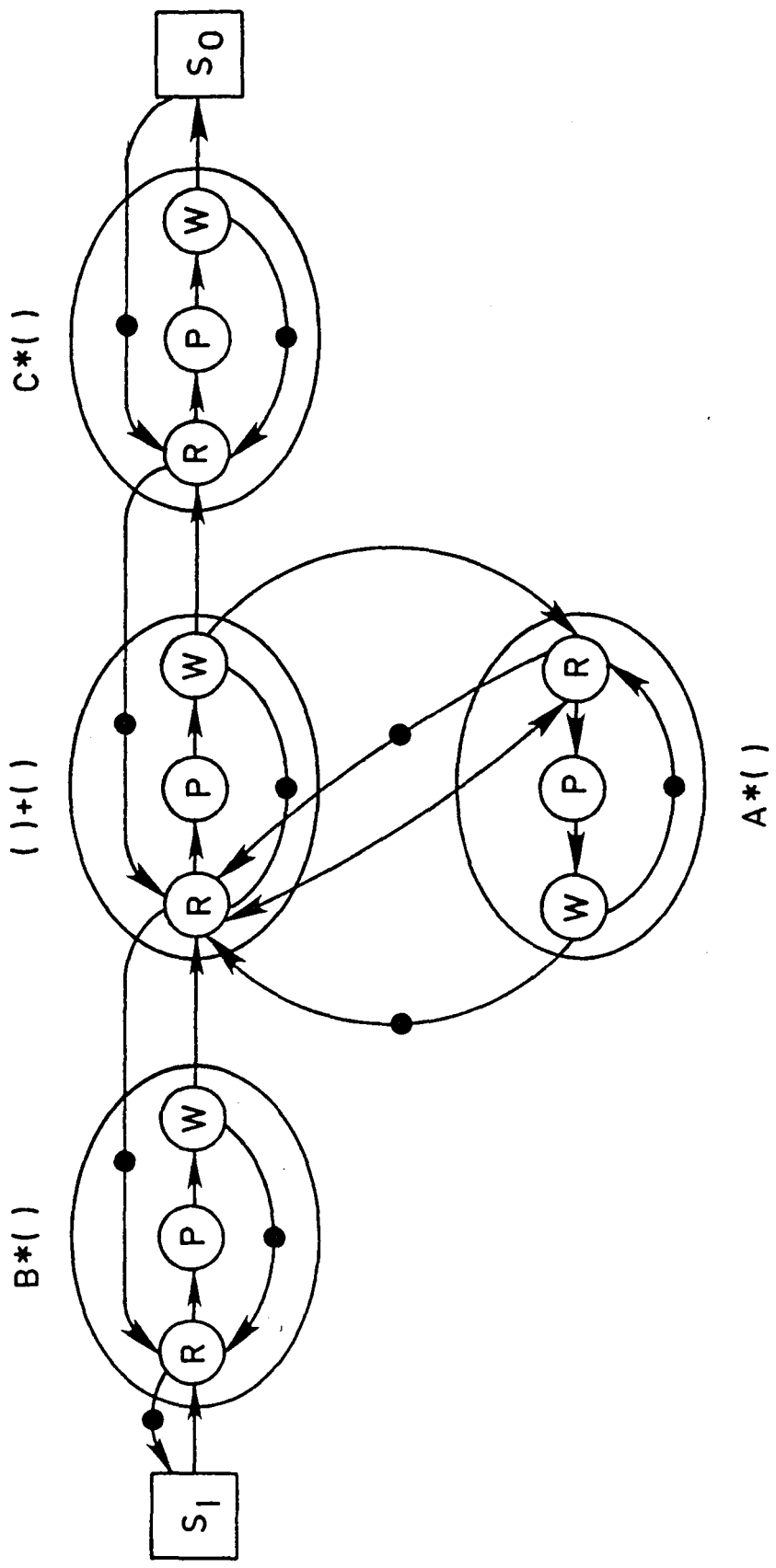
Figure 3. ATAMM computational marked graph model for discrete system equation.
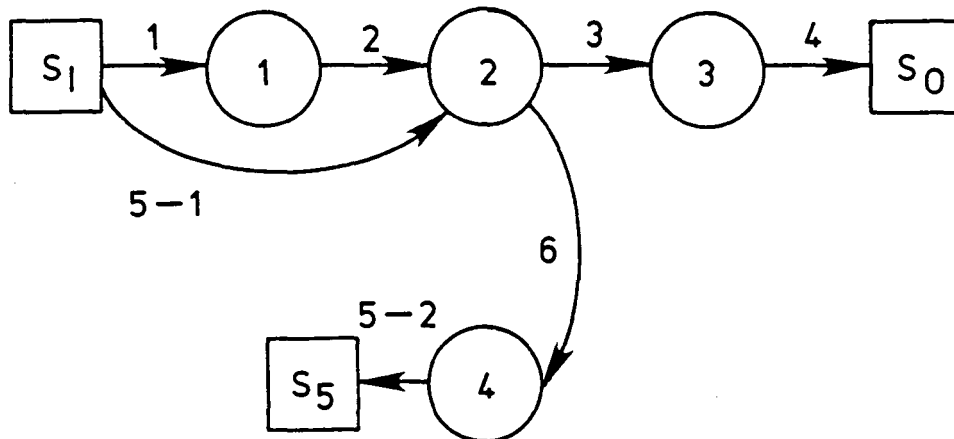
31
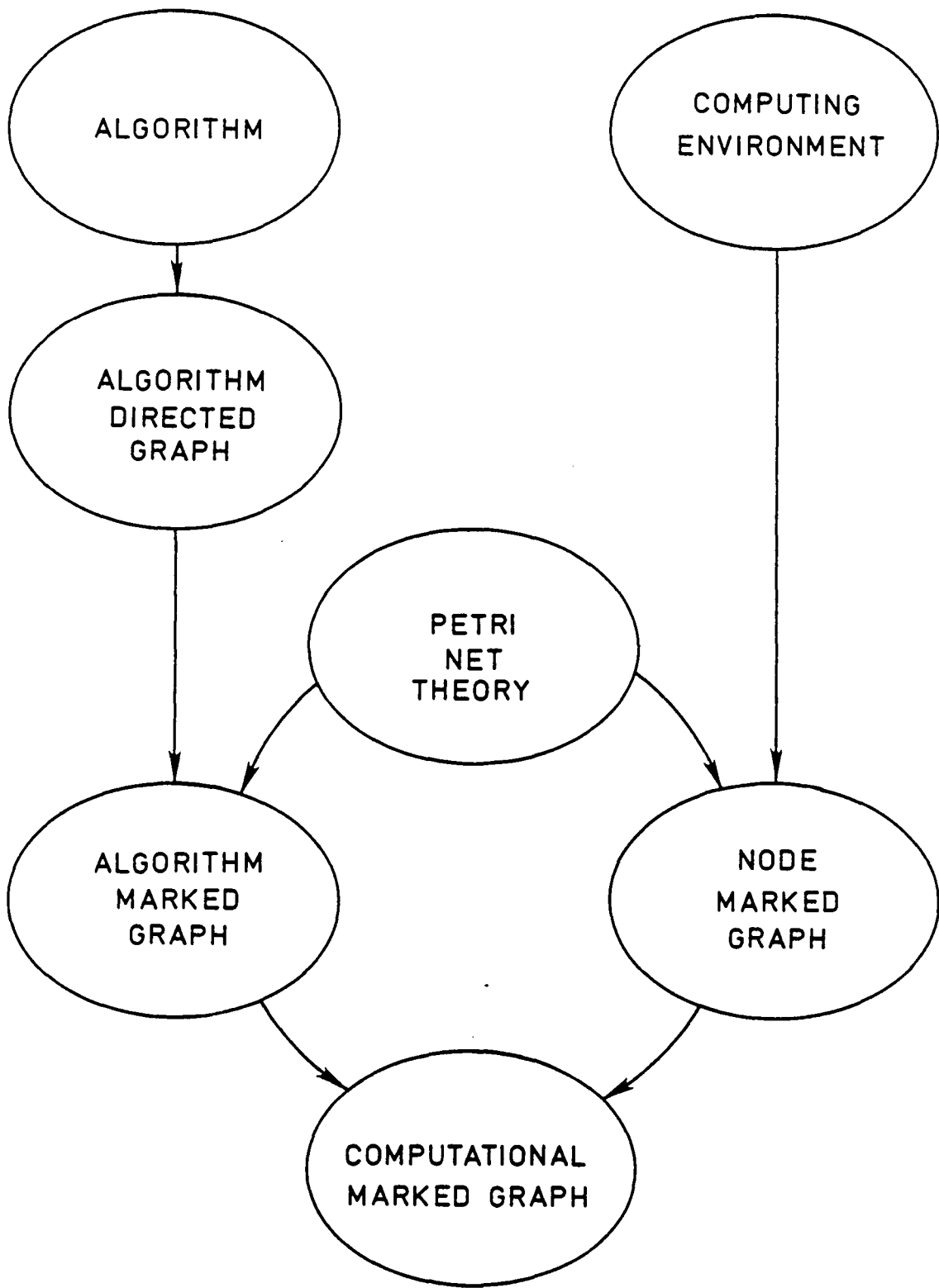
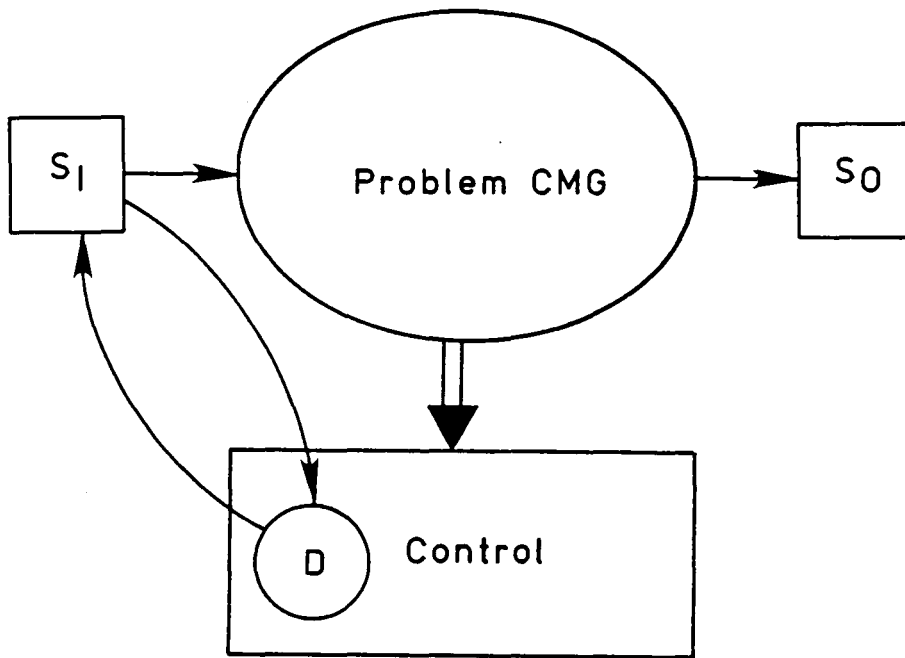Figure 4. ATAMM model components.

Figure 5. Modified algorithm graph for Figure 1.

Figure 6. Operating strategy implementation.
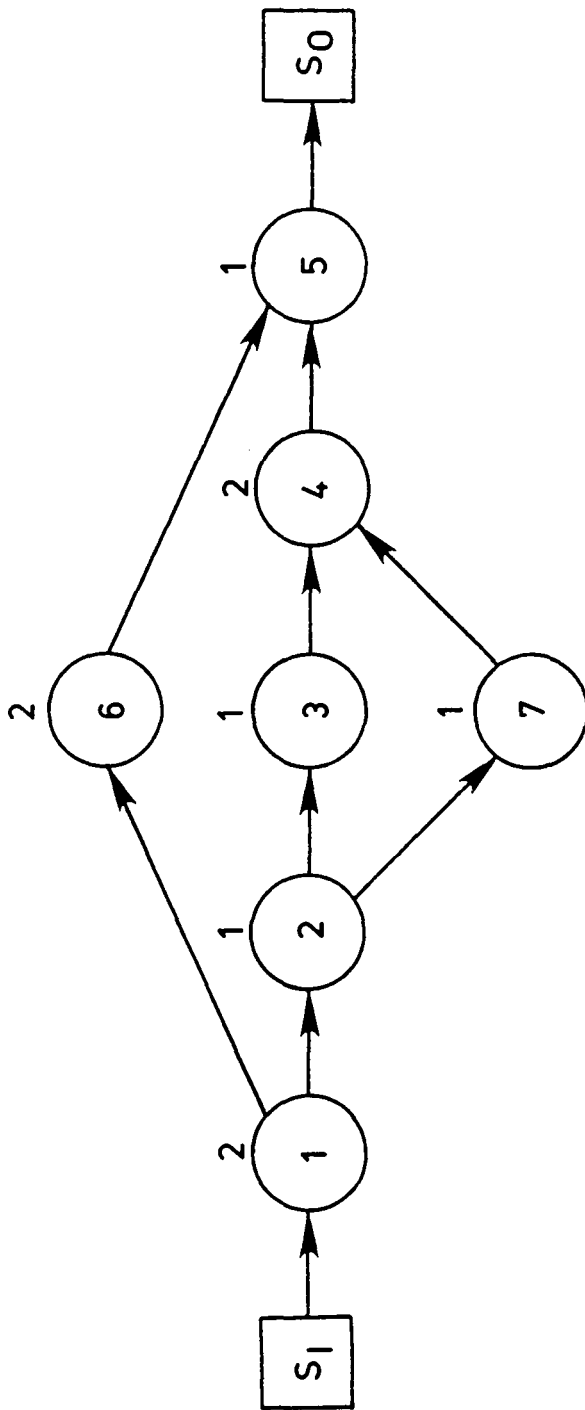
Figure 7. Algorithm graph for design example.
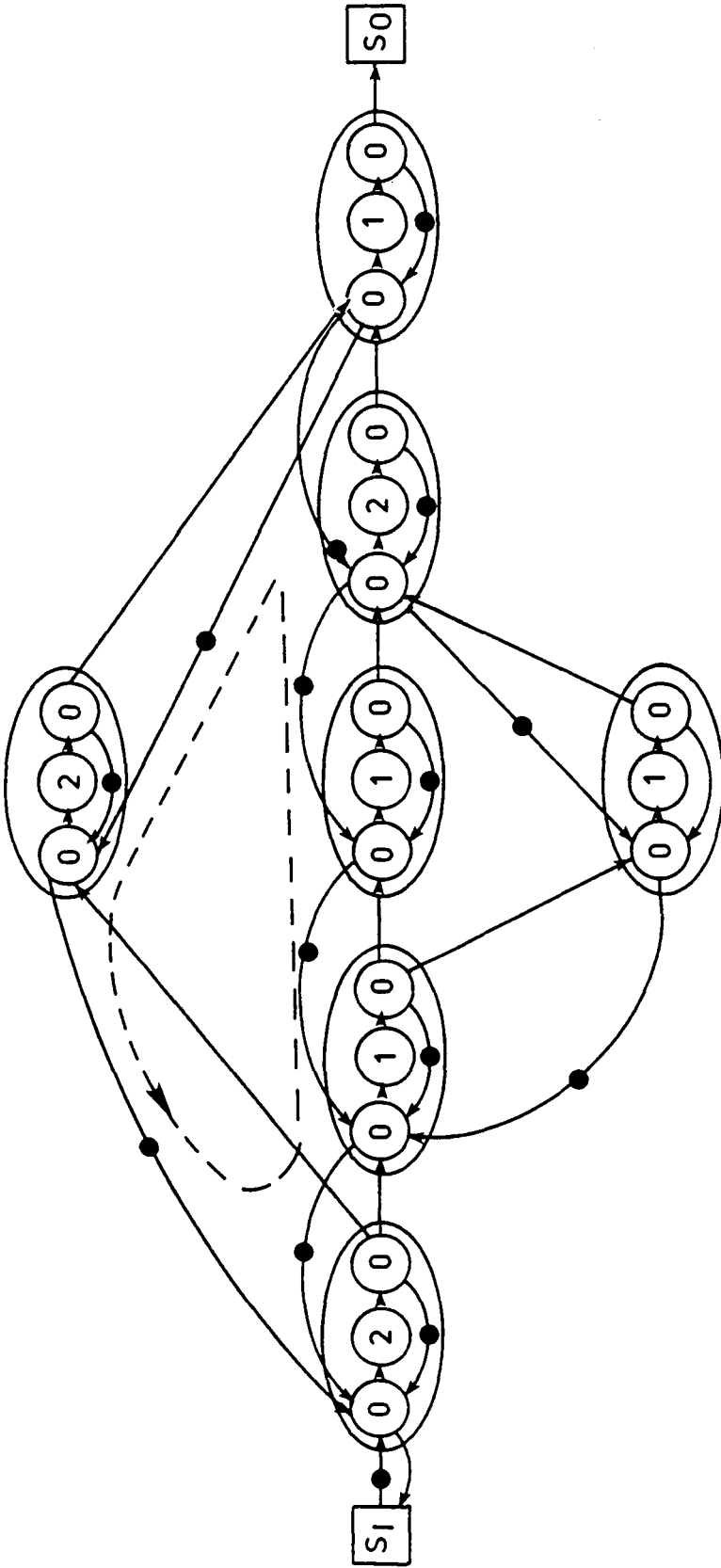
Figure 8. Computational marked graph for design example.
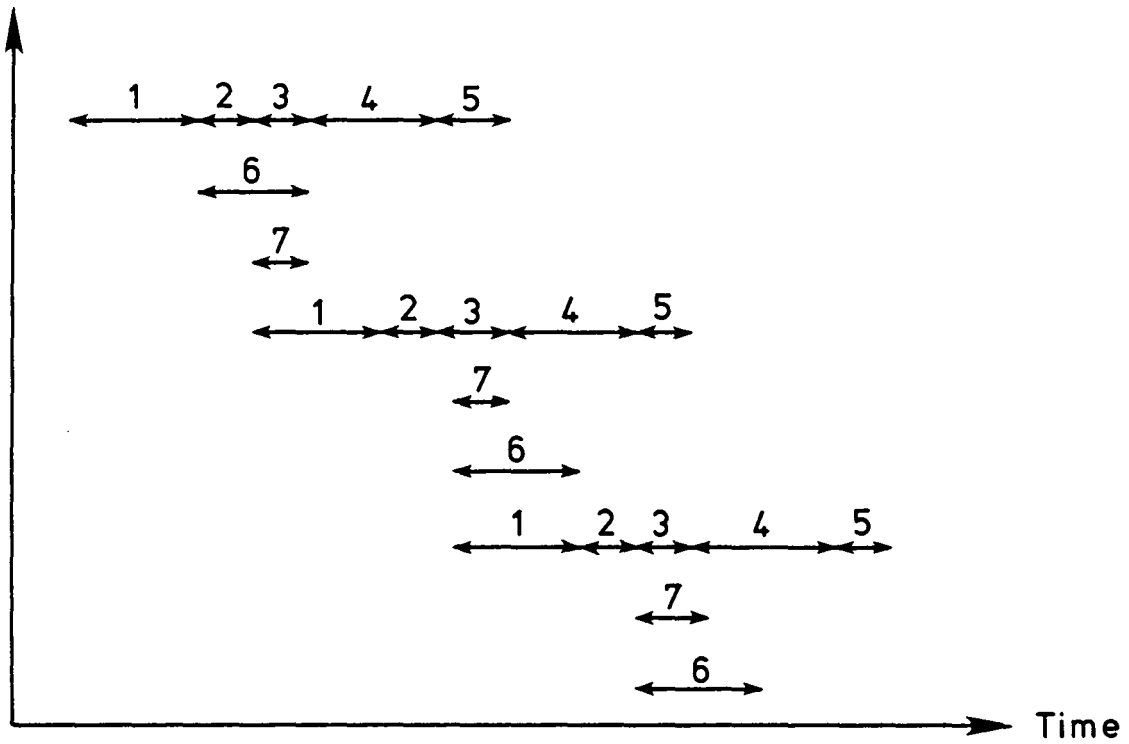
Figure 9. Graph play with TBO=3 and unlimited
functional units.
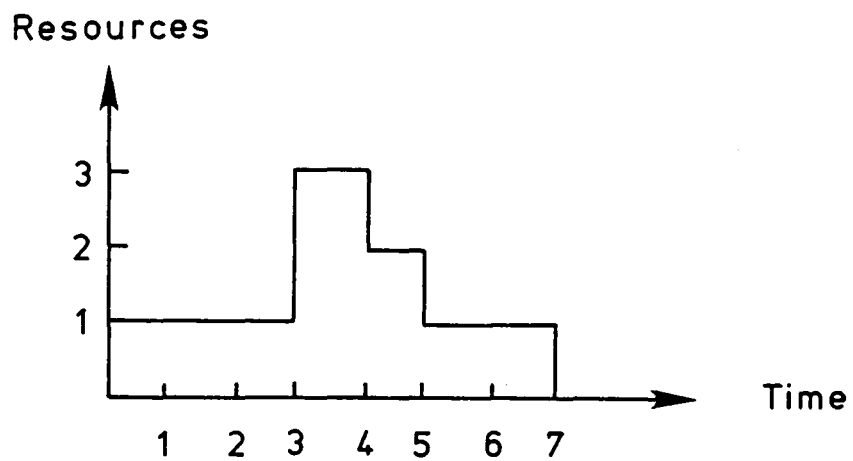
Figure 10. Resource utilization envelope
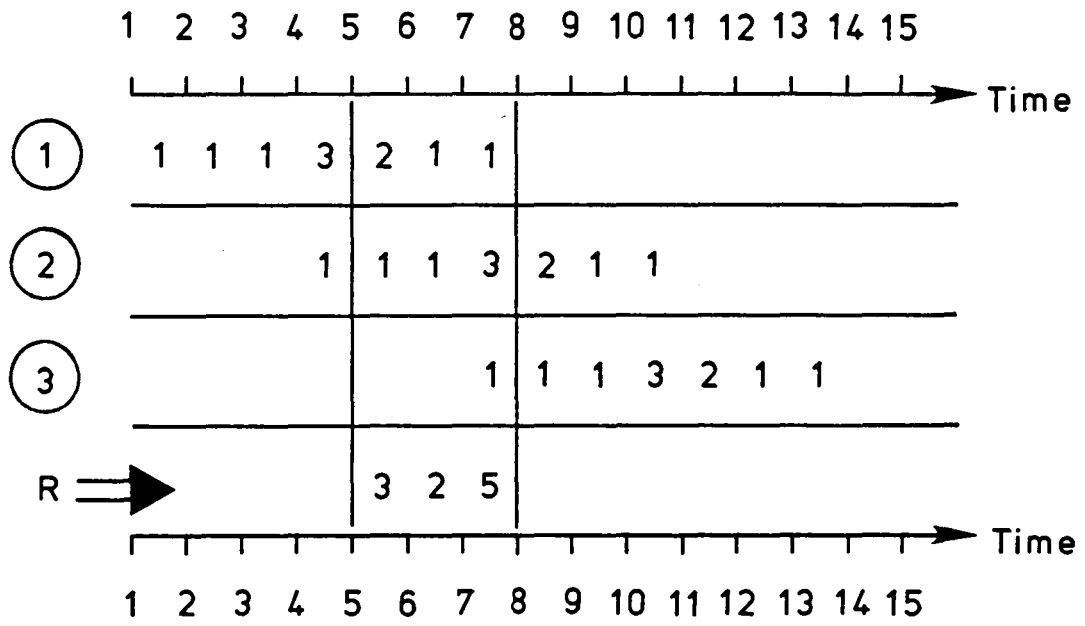for design example.
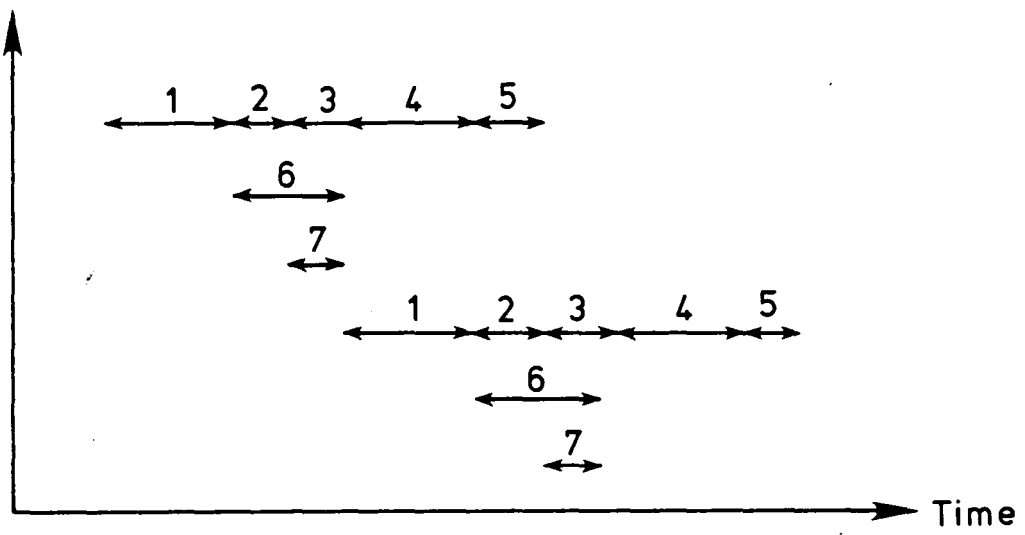
Figure 11. Graph play with TBO=4 and no control edges.
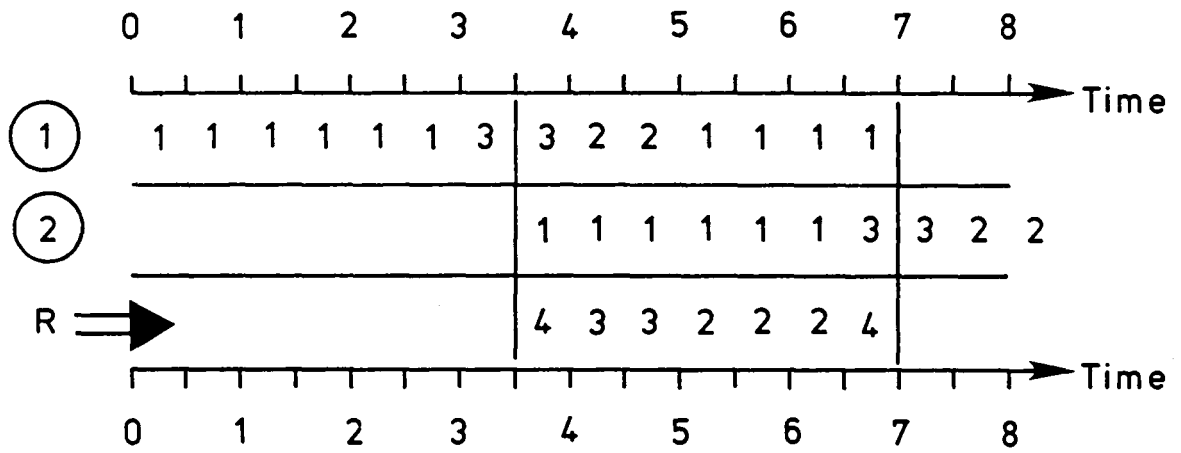
Figure 12. Resource envelope overlay diagram with TBO=3.
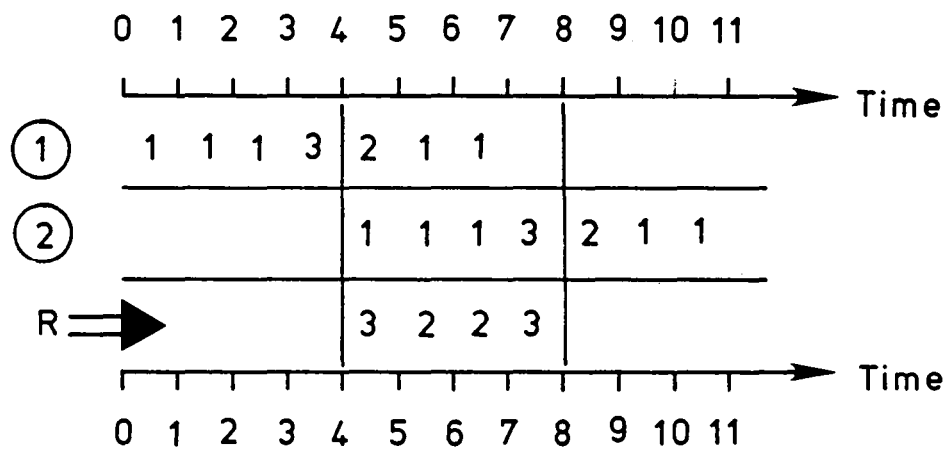
Figure 13. Resource envelope overlay diagram with TBO=3.5.

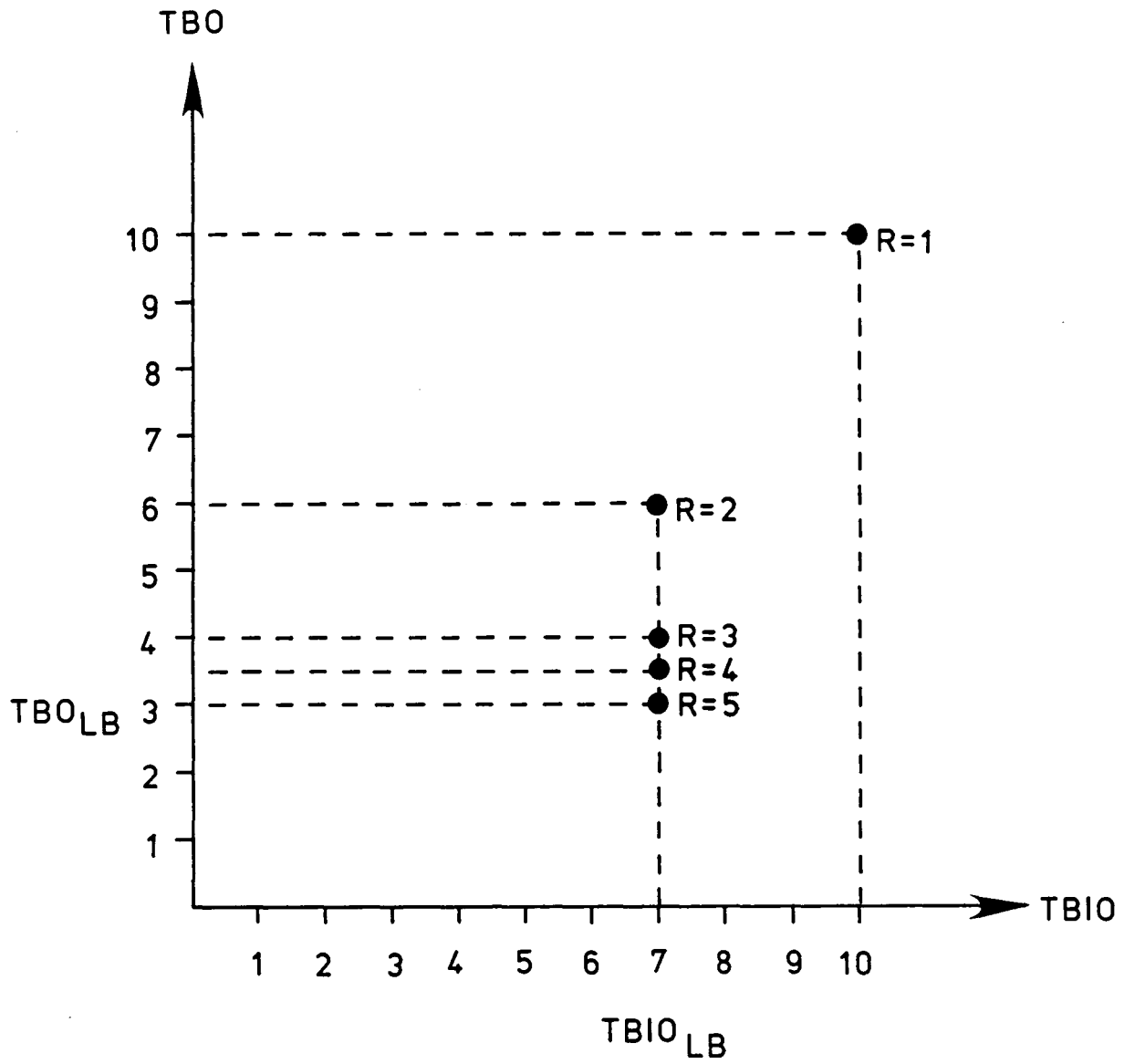Figure 14. Resource envelope overlay diagram with TBO=4.0.

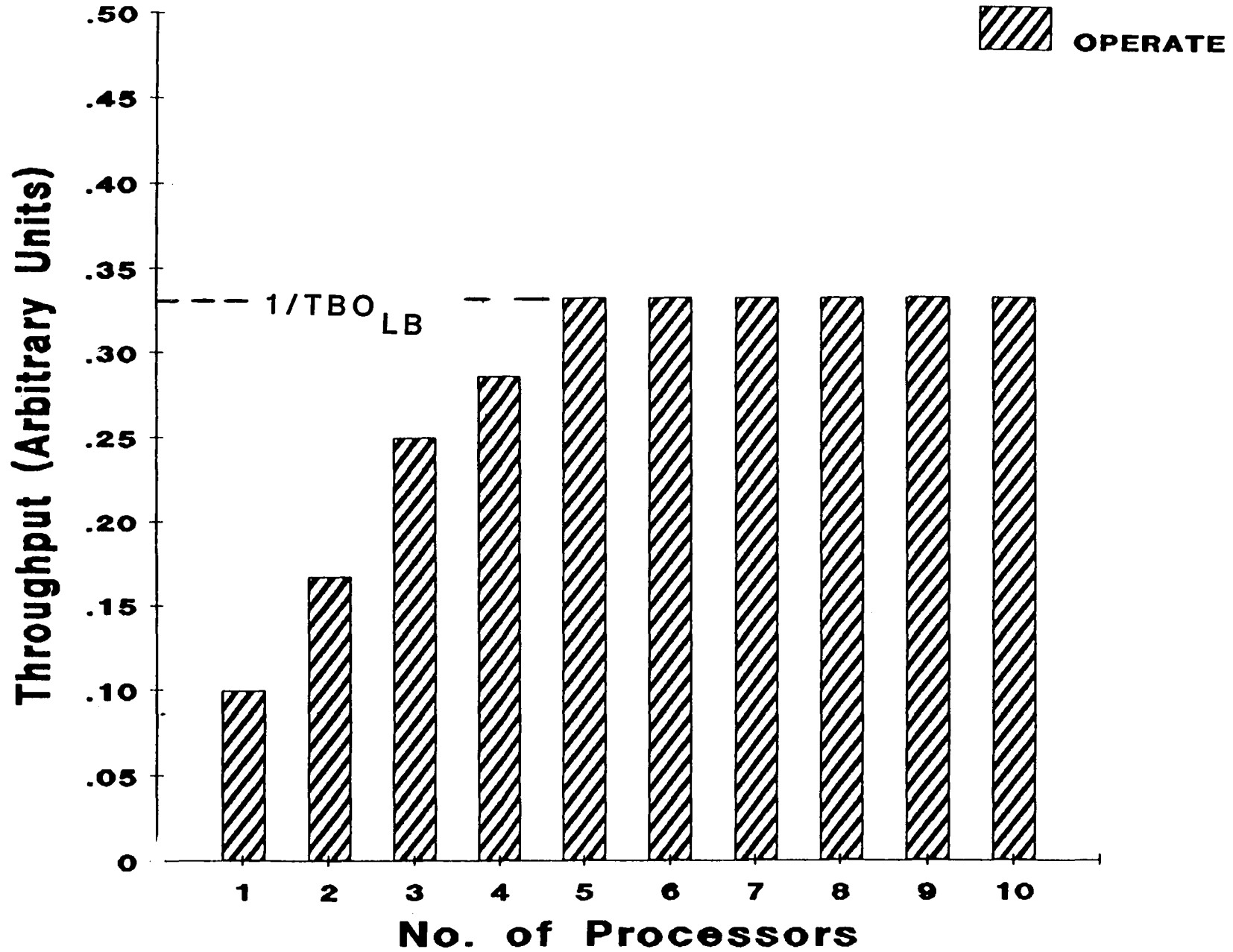Figure 15. Example algorithm graph performance analysis summary.

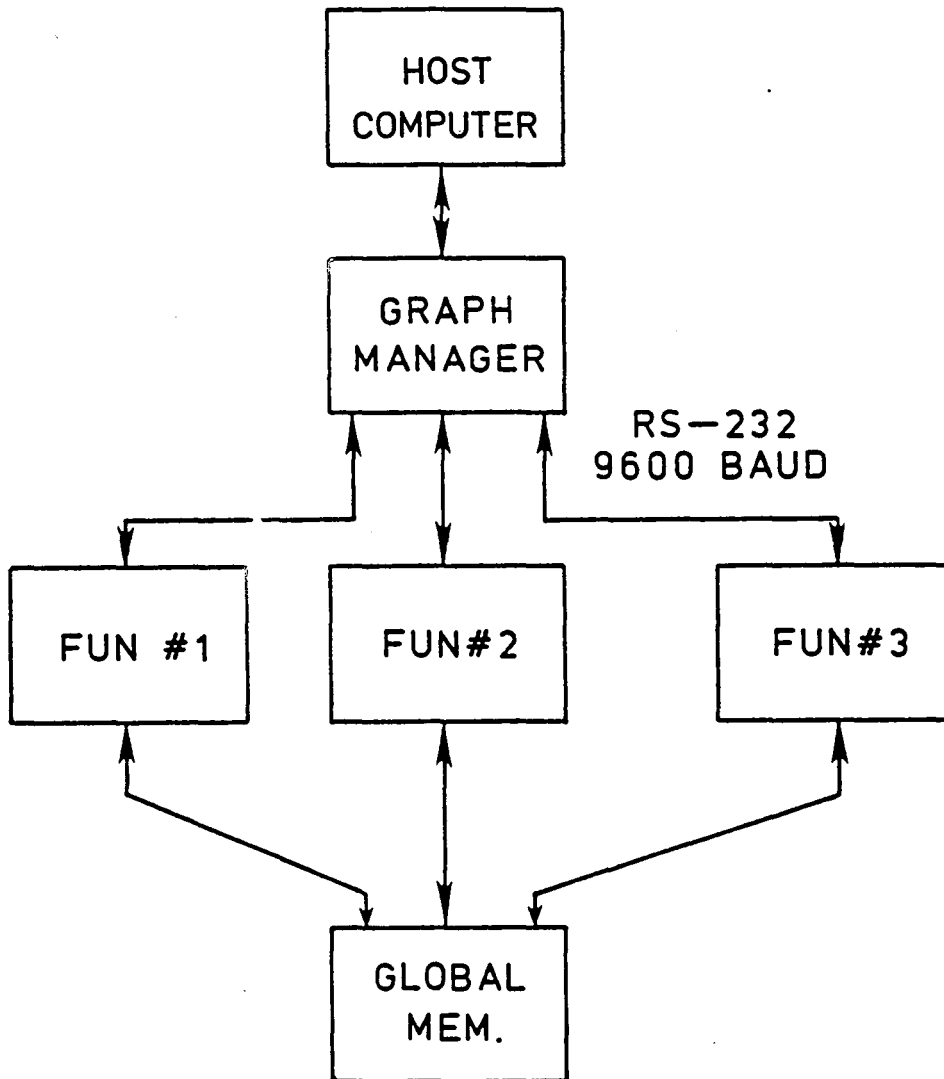FIGURE 16. PERFORMANCE MARGIN FOR EXAMPLE ALGORITHM.

Figure 17. Prototype hardware configuration for
ATAMM validation.

Report Documentation Page

1. Report No.	2. Government Accession No.	3. Recipient's Catalog No.
NASA CR-4167		

4. Title and Subtitle	5. Report Date
Modeling and Optimum Time Performance for Concurrent Processing	August 1988
	6. Performing Organization Code

7. Author(s)	8. Performing Organization Report No.
Roland R. Mielke, John W. Stoughton, and Sukhamoy Som	
	10. Work Unit No.
	584-02-11-01

9. Performing Organization Name and Address	11. Contract or Grant No.
Department of Electrical and Computer Engineering Old Dominion University Norfolk, Virginia 23508-0369	NAG1-683
	13. Type of Report and Period Covered

12. Sponsoring Agency Name and Address	
National Aeronautics and Space Administration Langley Research Center Hampton, Virginia 23665-5225	Contractor Report
	14. Sponsoring Agency Code

15. Supplementary Notes

Langley Technical Monitor: Paul J. Hayes

Interim Report
May 1987 - November 1987

16. Abstract

The development of a new graph theoretic model for describing the relation between a decomposed algorithm and its execution in a data flow environment is presented. Called ATAMM, the model consists of a set of Petri net marked graphs useful for representing decision-free algorithms having large-grained, computationally complex primitive operations. Performance time measures which determine computing speed and throughput capacity are defined, and the ATAMM model is used to develop lower bounds for these times. A concurrent processing operating strategy for achieving optimum time performance is presented and illustrated by example.

17. Key Words (Suggested by Author(s))	18. Distribution Statement
Data flow computers Algorithms to architecture mapping Petri nets Marked graphs Concurrent processing Large-grained algorithms	UNCLASSIFIED - UNLIMITED Subject Category 33

19. Security Classif. (of this report)	20. Security Classif. (of this page)	21. No. of pages	22. Price
Unclassified	Unclassified	48	A03

End of Document